A Comprehensive Model of a Novel Rotating Spool Compressor

International Compressor Engineering Conference at Purdue, July 16-19, 2012

Craig Bradshaw, PhD
Ray W. Herrick Laboratories and Cooling Technologies Research Center
West Lafayette, Indiana

Greg Kemp
Torad Engineering LLC
Alpharetta, Georgia

Joe Orosz
Torad Engineering
Alpharetta, Georgia

Eckhard Groll, PhD
Ray W. Herrick Laboratories and Cooling Technologies Research Center
West Lafayette, Indiana

A Comprehensive Model of a Novel Rotating Spool Compressor

Craig BRADSHAW[1], Greg KEMP[2*], Joe OROSZ[3], Eckhard GROLL[4]

[1] Ray W. Herrick Laboratories and Cooling Technologies Research Center, West Lafayette, IN 47907
Fax – (765-494-0787), E mail – cbradsha@purdue.edu

[2]Torad Engineering, 1005 Union Hill Road, Suite 2
Alpharetta, GA 30004
Phone – 678- 366- 3399, Fax – 678-366-3353, E mail – greg.kemp@toradengineering.com

[3]Torad Engineering, 1005 Union Hill Road, Suite 2
Alpharetta, GA 30004
Phone – 678- 366- 3399, Fax – 678-366-3353, E mail – joe.orosz@toradengineering.com

[4] Ray W. Herrick Laboratories West Lafayette, IN 47907
Fax – (765-494-0787), E mail – groll@purdue.edu

* Corresponding Author

ABSTRACT

A comprehensive simulation model of a novel rotating spool compressor is presented. The spool compressor provides a new rotating compression mechanism with easily manufactured components. Compared with other rotary compressors, the spool compressor presents the additional advantage of relocating the face sealing surfaces to the outer radius of the device. A detailed analytical geometry model of the spool compressor is presented which includes the geometry of the vane. This geometry model is included in a comprehensive model that includes sub-models for friction, leakage, and heat transfer. The results of the comprehensive model were validated using experimental data from a prototype compressor. The prototype compressor has an overall displacement of 23.9 cm^3, and was operated at rotational speeds between 1750 and 3250 rpm and pressure ratios between 2.1 and 2.9 using R410A as the working fluid. The model predicts the volumetric and overall isentropic efficiencies of the prototype compressor to within 6.3% and 11.2% MAE, respectively. The trends and spread in the data indicate that additional effort should be focused on the operation of the active sealing elements within the compressor.

1. INTRODUCTION

The rotating spool compressor is a novel rotary compressor mechanism most similar to the sliding vane compressor. Primary differences are described by Kemp et al. (2008, 2010) and include three key differences from a sliding vane compressor.
- The vane is constrained by means of an eccentric cam allowing its distal end to be held in very close proximity to the housing bore (typically less than 0.30mm) while never contacting the bore.
- The rotor has affixed endplates that rotate with the central hub and vane forming a rotating spool.
- The practical use of dynamic sealing elements to minimize leakage between the suction and compression pockets as well as between the process pockets and the compressor containment

These differences are shown in Figure 1 which presents a cutaway view of a rotating spool compressor with the key geometric features highlighted.
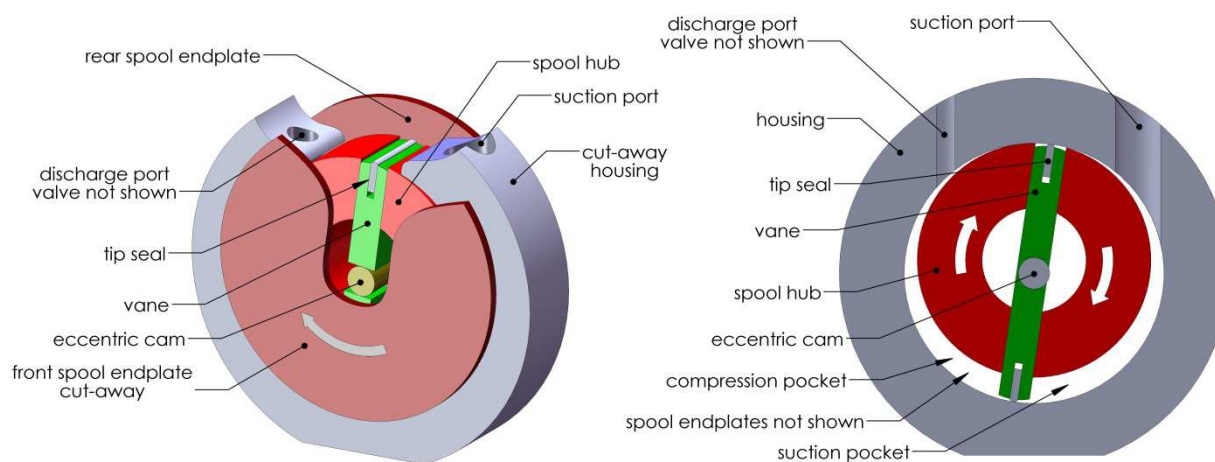
Figure 1: Cutaway view of rotating spool compressor mechanism with key components highlighted.

Due to the ever increasing need for increased performance envelopes and energy efficiency, air conditioning and refrigeration system technologies have greatly evolved over the last 30 years. Shortly after the inception of vapor compression systems, the market was dominated by two types of compressors, the reciprocating compressor for smaller cooling capacity systems and the centrifugal compressor for larger cooling capacity systems. This was dictated, for the most part, from a knowledge base and manufacturing capability (Soumeri, 2010). This gave way to various compressor designs implemented over the next 30 years that capitalized on newer manufacturing technology and met the ever increasing efficiency requirements dictated by regulation. By example ASHRAE 90.1 has mandated an improvement in chiller efficiency of 61% since 1977 while employing refrigerants with lower cycle efficiency (Lord, 2009). This has produced a current technical profile in the market that encompasses at least seven fundamental device types in various configurations with various optimum technical features.

More demand for higher efficiency components has resulted in a renewed interest in detailed compressor modeling to predict the performance of novel compressors. A recent approach to compressor modeling, called the comprehensive approach, has provided a complete analysis of positive displacement compressors. The comprehensive modeling approach relies on the unsteady mass and energy balance of a control volume, similar to that of Ooi and Wong (1997), with sub-models for each of the key physical phenomenon. Kim and Groll (2007) utilized the comprehensive approach for the modeling of a novel bowtie compressor. This type of compressor is based on the Beard-Pennock mechanism, which provides capacity control in a fixed volume device. Jovane (2007) applied the comprehensive approach to a novel rotary compressor, called a z-compressor. More recently, Mathison et al. (2008) developed a comprehensive model for a two-state rotary compressor, which provided insight into the optimum intermediate pressure for the best cycle and compressor efficiency. This work was continued by applying the approach to a rotary compressor with vapor injection as well as the novel rotary spool compressor (Mathison, 2011). Bell (2011) presented another recent addition to the applications of comprehensive modeling by examining the impact of oil flooding on scroll compressors. The comprehensive model provided a deeper insight into the unique internal performance of a scroll compressor flooded with oil. This allowed for a numerical optimization of scroll wraps for use in oil flooding, which may have been costly and time consuming to obtain experimentally. Finally, Bradshaw et al. (2011) applied the comprehensive modeling approach to a linear compressor for electronics cooling.

The variety of compressor types analyzed display the versatility of this modeling approach, which is why it is utilized in this work. First, an analytical model of the spool compressor geometry is presented, which will then be utilized in a comprehensive model. The results from this model are then compared against experimental results from a prototype compressor.

2. GEOMETRY MODEL OF A ROTATING SPOOL COMPRESSOR

The analytical expressions describing the spool compressor geometry are described in this section. Figure 2 shows simplified spool compressor geometry and identifies the polar coordinates used in the analysis. At any instant in the compressor rotation, the gas occupies either the suction, compression, or discharge chambers. These chambers are separated by the gate and the point referred to as Top Dead Center (TDC) as shown in Figure 2. This figure shows the center of rotation (point O), at the rotor center, the leading (point A) and trailing (point B) end of the compressor vane as well as the vane center (point C).
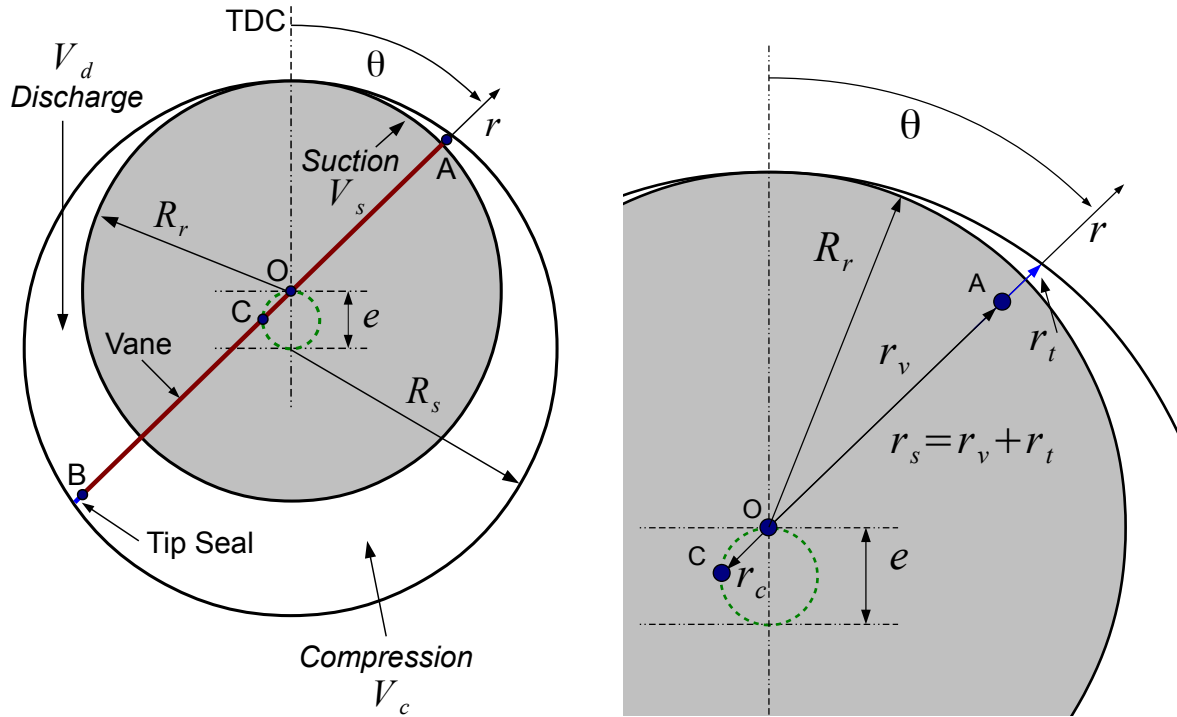

Figure 2: Simplified spool compressor planar geometry schematics highlighting global coordinates (left) and additional geometric vectors (right).

To calculate the volumes of the spool compressor a vector describing the position of the spool housing (stator) relative to the axis of rotation is developed. Utilizing the law of cosines, this vector can be written in terms of the housing radius and eccentricities, which are constants, and the angle of rotation of the rotor,

$$r_s = -e\cos\theta + \sqrt{e^2\cos^2\theta - e^2 + R_s^2} \tag{1}$$

where the lower limit of the eccentricity is given as:

$$e = R_s - R_r \tag{2}$$

Then, to identify the movement associated with the tip seals, the vector from point O to C is calculated as follows:

$$r_c = e\cos(\theta - \pi) \tag{3}$$

The vector describing the length of the vane as a function of rotor angle is described as,

International Compressor Engineering Conference at Purdue, July 16-19, 2012

$$r_v = R_v - r_c = R_g - e\cos(\theta - \pi) \tag{4}$$

where the length of the vane has an upper limit of,

$$R_v = \sqrt{R^2{}_s - e^2} \tag{5}$$

Finally, the vector describing the movement of the vane tip seal can be written as,

$$r_t = r_s - r_v \tag{6}$$

The vectors described above parameterize the key surfaces within a rotary spool compressor as a function of the rotor angle. Thus, the area of the suction, compression, and discharge chambers can be evaluated as a function of the rotor angle as well and calculated using:

$$A_s(\theta) = \int_0^\theta \frac{1}{2} r_s{}^2 d\theta - \int_0^\theta \frac{1}{2} r_r{}^2 d\theta$$

$$A_c(\theta) = \int_\theta^{\theta+\pi} \frac{1}{2} r_s{}^2 d\theta - \int_\theta^{\theta+\pi} \frac{1}{2} r_r{}^2 d\theta - A_s(\theta) \tag{7}$$

$$A_d(\theta) = \int_{\theta+\pi}^{2\pi} \frac{1}{2} r_s{}^2 d\theta - \int_{\theta+\pi}^{2\pi} \frac{1}{2} r_r{}^2 d\theta - A_c(\theta) - A_s(\theta)$$

for $0 < \theta < \pi$, and repeated for $\pi < \theta < 2\pi$. As the expression given in Equation (1) is unable to be integrated in closed form, the solution to each area integration is computed numerically using a finite difference method. Additionally, the rotor is slightly inset into the spool housing at the location of the TDC, this is known as the TDC relief. The depth of the TDC relief is an input to the geometry model and at these angular locations, $r_s = R_r$. Finally, the volume of each chamber can be computed by realizing that the geometry is planar,

$$V(\theta) = A(\theta) h_s \tag{8}$$

2.1 Spool Vane Geometry

The previous analysis assumes that the vane does not take up any of the volume within the compressor chambers. To account for this inaccuracy the following analysis is used to calculate the volume of the vane and tip seal within each chamber at each rotor angle. Figure 3 shows a close up of the vane geometry used for this analysis with the key dimensions identified.

The vane also employs planar geometry and thus, the vane analysis begins by calculating the area of the section of the vane that is within the rotor, which is fixed:

$$A_{v,r} = 2\tan^{-1}\left(\frac{\frac{1}{2} w_v}{R_r}\right) R_r^2 + w_v R_r \tag{9}$$
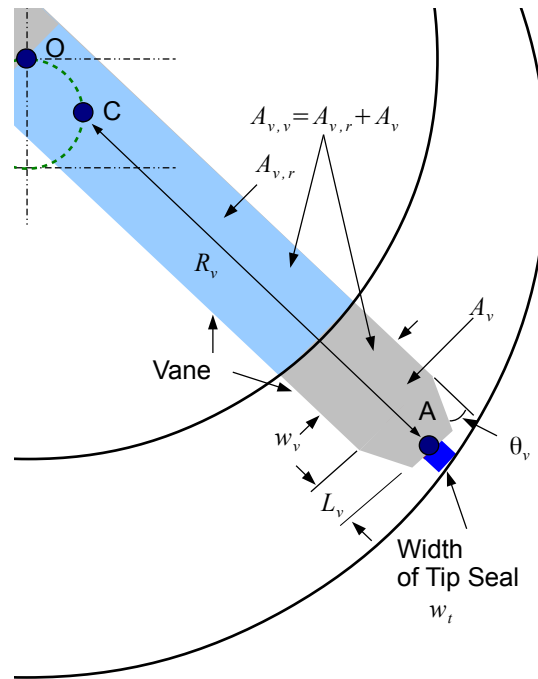
Figure 3: Close-up schematic of simplified spool vane and dynamic tip seal geometry included in model.

Then, the total variable area of the vane as it moves throughout the rotation, including the area within the rotor, is calculated as follows:

$$A_{v,v} = 2\left(R_v w_v - 2\left[\tfrac{1}{8}\left(w_v - w_t\right)^2 \tan\theta_v \right] + r_t w_t - r_c R_v \right) \tag{10}$$

Finally, since the only area of concern is the area pushed into one of the compressor chambers, the net gate area becomes:

$$A_v = A_{v,v} - A_{v,r} \tag{11}$$

where the area of the vane at point B is calculated in a similar way with the vectors offset by π. Using the gate area, the chamber volumes calculated in the previous section are modified as follows,

$$\begin{aligned}
V_s &= V_s - \tfrac{1}{2} A_v\big|_A h_s \\
V_c &= V_c - \tfrac{1}{2} A_v\big|_A h_s - \tfrac{1}{2} A_v\big|_B h_s \\
V_d &= V_d - \tfrac{1}{2} A_v\big|_B h_s
\end{aligned} \tag{12}$$

for $0 < \theta < \pi$, and repeated for $\pi < \theta < 2\pi$. Additional considerations for the situation when the vane passes through the TDC plane are also considered and included in the results but the analysis is omitted from this work for brevity.

The results of the geometry analysis are shown in Figure 4, which presents the final chamber volumes and rate of change of chamber volumes for each of the three chambers over one rotation of the spool rotor.
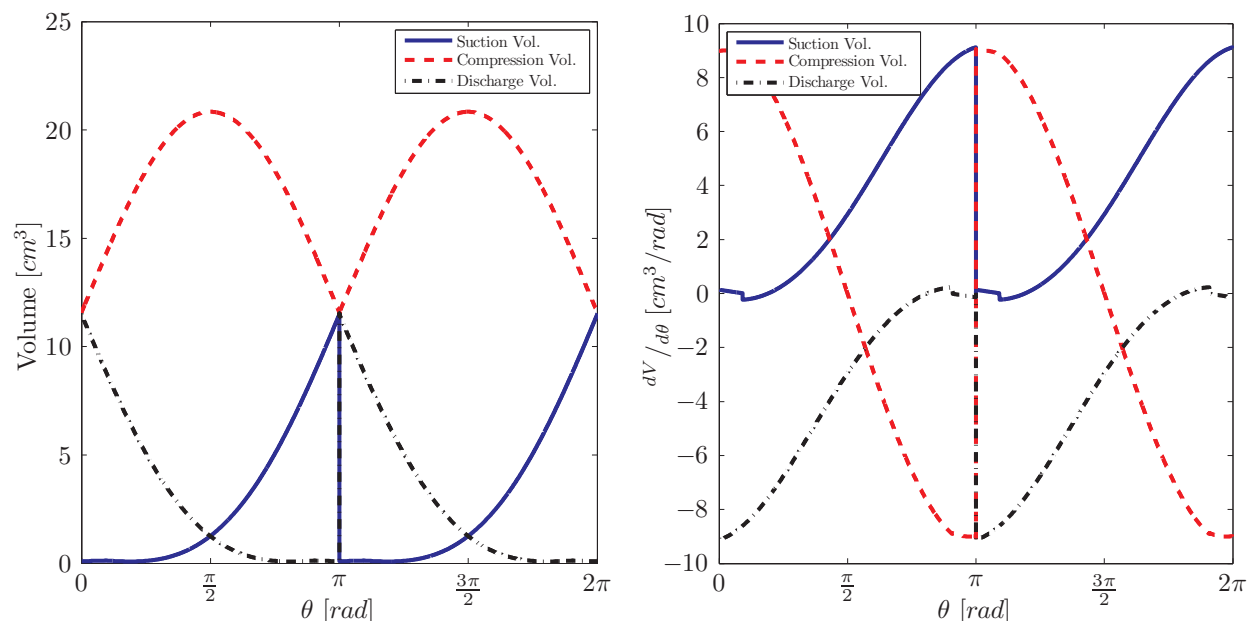
Figure 4: Results of spool geometry model, chamber volumes (left) and derivative of volume (right) as a function of rotor angle for spool compressor prototype RCP 4.2 as presented in Orosz et al. (2012).

Moving from the angle of 0 towards π, the suction volume initially starts near zero and displays a small expansion and compression prior to $\pi/2$, which is easier to observe in the right figure. This is a result of a combination of the TDC relief region and the vane geometry. The TDC relief region is the small region near the TDC plane that the spool housing is manufactured with the same radius as the rotor. This elongates the leakage gap across the TDC plane and reduces suction to discharge leakage. Since the radius of the stator and rotor are the same in this region the chamber volume is only impacted by the movement of the vane, which is beneath the rotor surface at this location. When the vane moves from TDC further into the suction chamber, past the TDC relief region, the vane begins to move out of the rotor, decreasing the volume, but the suction chamber begins to form as a result of the differences in radii of the rotor and stator. However, until roughly $\pi/4$, the movement of the vane dominates the chamber volume development which leads to a small compression volume before the suction process occurs.

The remaining suction process occurs until π, when the backside of the vane (point B) passes through the TDC plane and begins to generate another suction chamber. The gas in the previous suction chamber becomes the compression volume. This volume continues to expand until $3\pi/2$. Then, the chamber volume decreases until 2π, when the front side of the vane (point A) passes through the TDC plane. The compression chamber then becomes the discharge chamber as the back side of the gate (point B) rotates through another half rotation, pushing the gas out the discharge chamber. The process in all chambers is periodic about every half rotation and an entire process takes one and a half rotations to complete. Thus, for each rotation, two suction, compression, and discharge processes occur.

3. COMPREHENSIVE MODEL DEVELOPMENT

A comprehensive compressor modeling approach is utilized to predict the performance of the rotating spool compressor. This approach has been presented in detail previously for other positive displacement compressors (Bradshaw et al. 2011, Bell 2011, Mathison et al. 2008, 2011). The approach relies on a governing set of equations which are derived from a mass and energy balance within the working volumes of a positive displacement compressor:

$$\frac{d\rho}{d\theta} = \frac{1}{V}\left[-\rho \frac{dV}{d\theta} + \frac{1}{\omega}\left(\sum \dot{m}_{in} - \sum \dot{m}_{out}\right)\right] \tag{13}$$

$$\frac{dT}{d\theta} = \frac{-\rho h \dfrac{dV}{d\theta} - \left(uV + \rho V \dfrac{\partial u}{\partial \rho}\right)\dfrac{\partial \rho}{\partial \theta} + \dfrac{1}{\omega}\left(\dot{Q} + \sum \dot{m}_{in} h_{in} - \sum \dot{m}_{out} h_{out}\right)}{\rho V \dfrac{\partial u}{\partial T}} \tag{14}$$

These equations are enforced in each compressor chamber for each rotor angle. The equations also require inputs from a variety of sub-models including friction, leakage, valve, and heat transfer sub-models. The heat transfer sub-model utilizes a spiral heat exchange model to calculate the convective heat transfer coefficient. The correlation was developed for different geometries but it has been shown to be suitable for rolling piston compressors, which have a similar internal geometry to a spool compressor (Mathison, 2008). The valve model employed is a dynamic valve model with two modes of operation, as presented in Kim and Groll (2007) and Bradshaw et al. (2011). The friction models account for friction between the stator (housing) and rotor in the TDC relief region, from the tip seal on the stator (housing), and from the spool seals. An oil film shear model is utilized with the gap between each surface as an input to the friction and the leakage models.

3.1 Mass Flow and Leakage Models
Figure 5 shows a schematic of the 10 leakage paths accounted for in the model. The leakage paths across the TDC region and across the spool seals are modeled as compressible flow with friction (fanno flow), since the ratio of the leak path to height is high. All remaining leak paths are modeled as isentropic compressible flow through a nozzle. The leakage gap widths for the spool seals, tip seals, and TDC clearance were used to adjust the model results. Reasonable estimations for these gaps are known but they are difficult to measure accurately. The remaining leakage gaps are measured and this additional geometry information is used as inputs to the leakage model. The mass flow through the suction and discharge openings are also modeled as isentropic compressible flow through a nozzle.
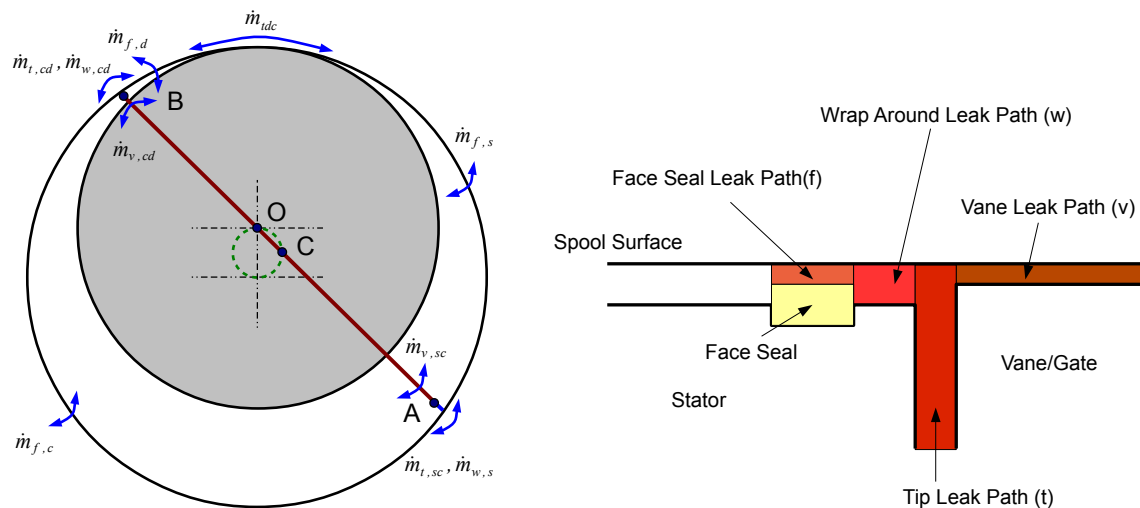

Figure 5: Schematic of leak paths considered in the comprehensive model, looking at the planar view (left) and the normal view (right).

4. MODEL RESULTS COMPARED WITH EXPERIMENTAL RESULTS

The comprehensive model results are compared with experimental data from the prototype spool compressor RCP 4.2 presented in Orosz et al. (2012), which has a displaced volume of 23.9 cm^3. This data was collected utilizing the

hot-gas bypass load stand also presented in Orosz et al. (2012). The compressor was operated at rotational speeds from 1750 to 3250 rpm and suction conditions at 905 kPa and 11 °C pressure and superheat, respectively, using R410A as the working fluid. The discharge pressure was varied to achieve pressure ratios between 2.1 and 2.9. Using the geometry presented in Section 2 and the overall model from Section 3 with the appropriate geometric inputs to represent RCP 4.2, the comprehensive model is compared to experimental data.

Figure 6 shows parody plots comparing the experimental volumetric and overall isentropic efficiencies compared with the model predicted values. The Mean Absolute Error (MAE) of each comparison is 6.3% and 11.2% for the volumetric and overall isentropic efficiencies, respectively.
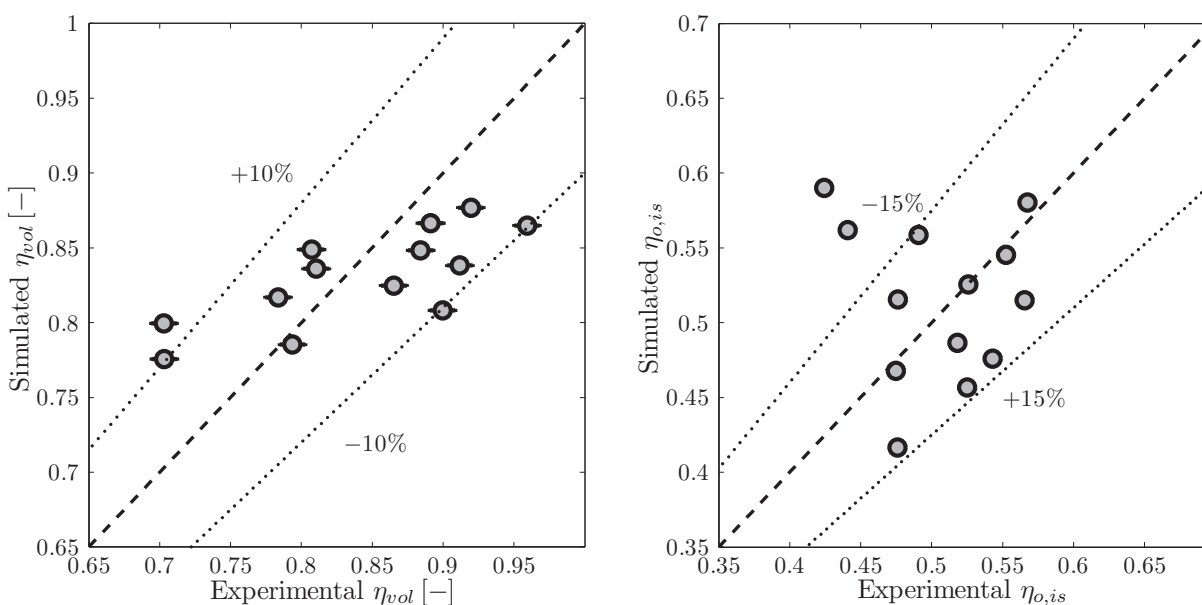

Figure 6: Model predicted volumetric (left) and overall isentropic (right, error within marker width) efficiencies of the prototype spool compressor.

The volumetric efficiency on the left of Figure 6 shows that while most points are predicted within 10% there is a trend in the error. This is indicative of the model not capturing all of the actual compressor behavior. The overall isentropic efficiency shows increased scatter and error. An increase in error in the overall isentropic efficiency is typical as this metric includes error from all of the sub-models combined. However, the amount of error in a small range of experimental efficiencies is also indicative of a trend in the actual performance that is not captured.

5. CONCLUSIONS AND FUTURE EFFORTS

An analytical model of the rotating spool compressor geometry is presented which includes the chamber volumes and the vane geometry. This model is incorporated into a comprehensive compressor model describing the rotating spool compressor. The model results are compared against test data collected using a prototype spool compressor at a variety of rotational speeds and operating conditions.

The comprehensive model predicts the volumetric efficiency within a reasonable amount of error. However, the trend in the error indicates that one or more of the sub-models do not accurately capture the behavior of the compressor. This is also seen in the overall isentropic efficiency where the error is exacerbated. While the trend is not obvious from this comparison the level of error indicates that there are still model inaccuracies.

Kemp et al. (2012, 2012a) presents results that indicate a high level of sensitivity of the experimental performance to changes of the design of both the spool seals and tip seals. Both seals are dynamic, activated seals, which are actuated by the pressure differentials created by the compressor. The leakage and friction sub-models assume that the spool seals and tip seals function the same regardless of the speed or operating condition. This behavior is inaccurate and the impact of an improved sub-model for both the tip seals and spool seals warrants further investigation.

NOMENCLATURE

A_c	Area of compression chamber, m^2		r_v	Vector describing position of vane tip, m
A_d	Area of discharge chamber, m^2		r_t	Vector describing position of tip seal, m
A_s	Area of suction chamber, m^2		r_c	Vector describing center of the vane, m
A_v	Area of vane within working chambers, m^2		T	Temperature, K
$A_{v,r}$	Area of vane within the rotor, m^2		u	Internal energy, kJ kg^{-1}
$A_{v,v}$	Total area of compressor vane, m^2		V_c	Compression chamber volume, m^3
e	Eccentricity of compressor, m		V_d	Discharge chamber volume, m^3
h	Enthalpy, kJ kg^{-1}		V_s	Suction chamber volume, m^3
h_s	Height of stator (housing), m		wt	Width of tip seal, m
$\dot{m}_{in}$	Mass flow in, kg s^{-1}		wv	Width of vane, m
$\dot{m}_{out}$	Mass flow out, kg s^{-1}		*Greek Letter*	
$\dot{Q}$	Heat transfer rate, W		θ	Rotor angle, rad
R_r	Radius of rotor, m		ρ	Density, kg m^{-3}
R_s	Radius of stator (housing), m		ω	Rotational speed, rad s^{-1}
R_v	Radius of vane, m			
r_r	Vector describing rotor surface, m			

REFERENCES

Bell, I. 2011. Theoretical and Experimental Analysis of Liquid Flooded Compression in Scroll Compressors. PhD thesis, Purdue University.

Bradshaw, C., Groll, E., Garimella, S. 2011. A comprehensive model of a miniature-scale linear compressor for electronics cooling. International Journal of Refrigeration. 34(2011), 63-73.

Jovane, M. 2007. Modeling and analysis of a novel rotary compressor. PhD thesis, Purdue University.

Kemp, G., Elwood, L., Groll, E., 2010. Evaluation of a Prototype Rotating Spool Compressor in Liquid Flooded Operation. In: Proceedings of the International Compressor Engineering Conference. Purdue University, West Lafayette, IN USA. No. 1389.

Kemp, G., Garrett, N., Groll, E., 2008. Novel Rotary Spool Compressor Design and Preliminary Prototype Performance. In: Proceedings of the International Compressor Engineering Conference. Purdue University, West Lafayette, IN USA. No. 1328.

Kemp, G., Orosz, J., Bradshaw, C., Groll, E., 2012. Spool Compressor Tip Seal Design Considerations and Testing. In: Proceedings of the International Compressor Engineering Conference. Purdue University, West Lafayette, IN USA. No. 1258.

Kemp, G., Orosz, J., Bradshaw, C., Groll, E., 2012. Spool Seal Design and Testing for the Spool Compressor. In: Proceedings of the International Compressor Engineering Conference. Purdue University, West Lafayette, IN USA. No. 1259.

Kim, J., and Groll, E. 2007. Feasibility study of a bowtie compressor with novel capacity modulation. International Journal of Refrigeration, 30(8):1427-1438.

Lord, R., 2009. System Level Efficiencies and Strategy to Enable their Use and Improvement. Technical Report, Carrier Corp.

Mathison, M., Braun, J., Groll, E. 2008. Modeling of a two-stage rotary compressor. HVAC&R Research, 14(5):719-748.

Mathison, M. 2011. Modeling and Evaluation of Advanced Compression Techniques for Vapor Compression Equipment. PhD thesis, Purdue University.

Ooi, K., and Wong., T. 1997. A computer simulation of a rotary compressor for household refrigerators. Applied Thermal Engineering, 17(1):65-78.

Orosz, J., Kemp, G., Bradshaw, C., Groll, E., 2012. Performance and Operating Characteristics of a Novel Rotating Spool Compressor. In: Proceedings of the International Compressor Engineering Conference. Purdue University, West Lafayette, IN USA. No. 1257.

Soumerai, H.., 2010. History in the Air Conditioning and Refrigeration Industry: Breakthrough of Large Positive Displacement Rotary Compressors in the Second Half of the 20th Century. ASHRAE Web Publication; A Look Back at HVAC&R.